LONG-TERM EROSION DOWNSTREAM REGULATOR STRUCTURE

K. S. El-Alfy[1], M. N. Hammed[2], A. M. Talaat[2], and A. F. Yuossif [3]

[1] Assist Prof., Irrigation & Hydraulics, Dept., Faculty of Eng., Mansoura University, Egypt
[2] Prof. of irrigation and hydraulics, Faculty of Engineering, Ain Shams University, Egypt
[3] Prof. of Soil Mechanics and Foundations, Faculty of Engineering, Menoufia University, Egypt

ABSTRACT

The correct design of the regulator structure requires complete prediction of the ultimate dimensions of the scour hole profile formed downstream the solid apron. In the following study a mathematical model is developed to predict the ultimate dimensions of the scour hole profile formed downstream the solid apron of the regulator structure under various operating conditions. These parameters are, the maximum predicted scour depth, its distance from the apron of the regulator, and the total length of the scour hole formed directly downstream the solid apron of the regulator. A laboratory model is built-up to study the long-term scour depth under various operating conditions. Both the long-term scour depth and scour hole profile are measured. The effect of the bed material median diameter is also included. The laboratory results are used in verification of the developed mathematical model resulted from the theoretical study of the problem. It is found that the long-term scour depth depends mainly on the jet diffusion characteristics, Shields parameter, Reynolds number, and densemeteric Froude number. From the laboratory results, it is evident that the results from the mathematical model are very close to the corresponding results from the experimental work for different bed material median diameters.

INTRODUCTION

An understanding of local scour phenomenon is very important for the safety and integrity of the regulator structure. The magnitude, location, and shape, of the scour hole occurring downstream the hydraulic structures is a function of dynamic and physical characteristics of the riverine system. The most dangerous local scour takes place during the refilling of the canals after the annual maintenance period. At refilling of the canals the tail water depth downstream the regulator structures is so small that it is not sufficient for the sequent depth of the hydraulic jump confirmation on the solid floor, which has the responsibility for the energy dissipation of the flowing water.

The short-term scour downstream the solid apron of the regulator vent during the refilling of the canals was studied by Mohammed [8]. A steady state short-term scour model was developed to predict the short-term scour hole dimensions downstream the solid apron. He used a laboratory flume of 4.0 m. length, 0.42 m. width, and 0.2 m. depth. He concluded that the using of midstream flow divider causes the jet and the scour hole more symmetrical. He also concluded that the short-term scour depth in a rectangular channel is caused mainly by the attached jet phase, and depends mainly on the Froude number at the end of the solid apron, the discharge, and the particle size of the bed material.

In 1992 Kamel [5] studied the effect of supercritical flow on riprap protection downstream the weir structure. She studied the effect of the flow conditions on riprap protection downstream the solid apron. The effect of the seepage on riprap protection is also studied. The study was carried out through experimental and theoretical approaches. She concluded that, there is a reverse relation between the stability of the riprap downstream the solid apron and the discharge; there is a direct logarithmic relation between the scour depth and the time; the seepage force increases the tendency of particles to move from the scour hole especially under the high water head; and the Froude number had an important effect on the maximum scour depth.

THEORETICAL STUDY

INITIATION OF MOTION OF BED MATERIAL

The particles initiate motion when the shear stress of the flowing water becomes greater than the critical shear stress of the bed material. According to Kramer [4], the motion of bed material can be classified into three types:

- Weak movement : a few particles are in motion.
- Medium movement : the particles of d_{50} begin to move.
- General movement : this occurs when all particles are in motion.

In researches carried out by many researchers such as Schoklitch [10], Kramer [4], Shields (1936), etc., it is mentioned that in reality there is no truly a critical condition for initiation of motion for which motion begins suddenly as the condition is reached.

THE EQUILIBRIUM OF A SINGLE PARTICLE ON A MOBILE BED

When the water flowing over a mobile bed, it creates forces on the bed grains. These forces tend to move particles or increase its stability. The forces acting on a particle of bed material under turbulent flow are:

a- Submerged weight of the particle $F_g = C_3 \gamma_s D_s^3$

b- Lift force $F_L = C_L C_4 D_s^2 \rho \frac{U^2}{2}$

c- Drag force $F_d = \tau_0 C_5 D_s^2$

where

- C_L lift coefficient
- C_3 form coefficient related to the volume of particle = $\pi\pi/6$ for spherical shape
- C_4 form coefficient related to the effective surface of the particle in the direction of the lift force
- C_5 form coefficient defining the effective surface of the particles
- D_s median diameter of grains
- D average diameter of grains
- U velocity of flow near the bed
- γ_s specific weight of solid particles
- τ_0 bed shear stress

When the shear stress produced by the resultant forces in direction of the flowing water exceeds the critical shear stress, the particles start motion. As stated by Simons, and Senturk,, 1976, for a fully developed turbulent flow the equilibrium of a single particle can be treated as the following equation [11]:

$$a_1C_3(\gamma_s - \gamma)D_s^3 \sin(\theta\theta - \varphi) - a_1C_LC_4D_s^2 \rho \frac{U^2 \sin\theta}{2} = a_1\tau_0C_5D_s^2 \cos\theta \qquad (1)$$

where

- a_1 distance between points C and G
- C the point of the center of gravity
- G the point of support of the particle

According to Brahms 1753 (cited from Simon [11]), the shear stress is proportional to the velocity near the bed $\tau = \rho U_*^2$, U=KU$_*$. At the critical condition (at the initiation of motion) τ_0 in Equation (1) equals to τ_c then;

$$C_3(\gamma_s - \gamma)D_s \sin(\theta\theta - \varphi) - C_LC_6 \tau_c \sin\theta = C_5\tau_c os\theta \qquad (2)$$

where $C_6 = C_4 K^2/2$; then

$$\tau_c = \frac{C_3(\gamma_s - \gamma)D_s \sin(\theta - \varphi)}{C_LC_6 \sin\theta + C_5 \cos\theta} \qquad (3)$$

For horizontal bed i.e. $\phi = 0$

$$\tau_c = \frac{C_3(\gamma_s - \gamma)D_s}{C_LC_6 + C_5 \cot\theta} \qquad (4)$$

The initiation of motion has been studying by many researchers. They concluded that the beginning of motion of the bed material is a function of the dimensionless number; $\tau_c/(\gamma_s - \gamma)D_s$. Egiazaroff [1] developed his equation that controlling the incipient motion for a mixture of nonuniform particles as follows:

$$\frac{\tau_c}{(\gamma_s - \gamma)D_{50}} = \frac{0.1}{[\log \frac{D_{50}}{D^-}]} \qquad (5)$$

where D^- is the average diameter of grains

In 1936 Shields (cited from Simon [11]) developed the well-known graphical presentation between $\tau_c/(\gamma_s-\gamma)D_s$ and $U_* D_s/\nu$, which is known as Shields diagram. The first term is often referred as Shields parameter, and the second term is the boundary Reynolds number; $\frac{D}{\nu}\sqrt{0.1(\gamma_s/\gamma-1)gD_s}$ which depends mainly on grains characteristics.

STUDY OF LONG-TERM SCOUR

The digital computer is used to simulate the behavior of the long-term scour by applying the necessary theories to describe the physical process in terms of dependent and independent variables and by specifying the necessary functional relationships to describe the physical system. The flowchart of the computer program that describes the long-term scour is illustrated in Appendix.

The jet in the scour hole is treated as a plan jet extending at a ratio;

$$C_1 = ds/L_{sm} \tag{6}$$

where

d_s is the long-term scour depth
L_{sm} is the distance between the apron end and the section of maximum scour

At the state of bed equilibrium, i.e. the depth of the scour hole becomes approximately constant; the applied shear equals the resistance shear.

$$\tau_0 \text{ (applied shear)} = \tau_0 \text{ (resistance)} \tag{7}$$

Due to the Rajaratnam theory, 1976 the eddy viscosity in the expanding jet is

$$\varepsilon_m = C_2 X U_m \tag{8}$$

where

C_2 is constant due to Hoffmans [3] equals 0.0035-0.004
U_m is the maximum velocity

and

$$U_m = K.U_{av} \tag{9}$$

where

U_{av} is the average velocity at the maximum scour section
K constant

Then the applied shear stress $\tau_0 = \rho\varepsilon_m \frac{dU}{dy}$, which can be approximated to;

$$\tau_0 = \rho\varepsilon_m \frac{U_{av}}{d_s} \tag{10}$$

The continuity equation between the jet section at the end of the apron and the maximum long-term scour location is:

$$U_{av}.d_s = U_a \,.Y_a \tag{11}$$

where

U_a jet velocity at the end of the apron
Y_a flow depth at the end of the apron

Substituting Equation (11) in Equation (10) then,

$$\tau_0\ (applied\ \ shear) = \rho\varepsilon_m \frac{U_a Y_a}{d_s^2} \tag{12}$$

According to Shields initiation of motion (1936);

$$\tau_0\,(resis\tan ce) = C_s(S_s - 1)D_g\gamma_w \tag{13}$$

Equating Equations (12) and (13) as in Equation (7), it follows:

$$\rho\varepsilon_m \frac{U_a Y_a}{d_s^2} = C_s(S_s - 1)D_g\gamma_w \tag{14}$$

$$d_s = \left[\frac{\rho\varepsilon_m U_a Y_a}{C_s(S_s - 1)D_g\gamma_w}\right]^{0.5} \tag{15}$$

from Equation (8)

$$\varepsilon_m = C_2 \text{ X } U_m \tag{16}$$

from continuity between the end of the apron and the section of the maximum scour depth

$$U_a\ Y_a = U_m\ d_s \tag{17}$$

substitute Equation (17) in Equation (16), then

$$\varepsilon_m = C_2 \frac{Y_a U_a X}{d_s} \tag{18}$$

at the section of the maximum long-term scour X= L_s ;

$$\varepsilon_m = C_2 \frac{Y_a U_a L_s}{d_s} = C_2 U_a Y_a \left[\frac{L_s}{d_s}\right] \tag{19}$$

substitute ε_m from Equation (19) in Equation (15) leads to;

$$d_s^2 = \left[\frac{\rho C_2 U_a^2 Y_a^2}{C_s(S_s - 1)D_g\gamma_w}\right]\frac{L_s}{d_s} \tag{20}$$

from Equation (6) $1/C_1 = L_s/d_s$ then;

$$d_s^2 = \left[\frac{C_2 U_a^2 Y_a^2}{C_s (S_s - 1) D_g g C_1} \right] \tag{21}$$

$$\frac{d_s^2}{Y_a^2} = \left[\frac{C_2 U_a^2}{C_1 C_s (S_s - 1) D_g g} \right] \tag{22}$$

$$\frac{d_s}{Y_a} = \sqrt{\frac{C_2}{C_1 C_s}} \frac{U_a}{\sqrt{(S_s - 1) D_g g}} \tag{23}$$

From Shields diagram, Simons and Senturk [11] stated that at the region of fully developed turbulent flow, the value of $C_s = \tau_c / (\gamma_s - \gamma) D_{50}$ is independent of Reynolds number and equals to 0.06. Meyer-Peter and Mueller (cited from Simon [11]) suggested a value of 0.047 instead of 0.06; but Simons and Senturk, stated that the value of 0.06 is most generally accepted. The values of C_1 and C_2 can be computed from laboratory data. Then the long-term scour depth can be calculated as illustrated in computer program flowchart shown in Appendix.

EXPERIMENTAL WORK

The experimental determination of the physical parameters of the scour hole occurring downstream the solid apron of regulators under high values of Froude number were used in the verification of the theoretical solution of the phenomenon. In this study the values of Froude number range between 3.0 and 9.5. The Experiments were conducted in a recirculating tilting flume built-up in the laboratory of Irrigation and Hydraulics, Menoufia University. It is a closed operating system with the following characteristics, 17.6 m overall length, cross-section of 0.6 m x 0.6 m, upstream tank of 1.50 m. head, and a discharge ranges from 10 to 41 liter/sec. The shape and the general arrangement of the flume are shown in Figure (1).

The first set of the experiments was carried on a mobile bed of median diameter of 10.0 mm. It consists of seventeen runs. These runs were divided into three categories according to the upstream water head. The first category was carried out under upstream water head ranges from 108 cm to 113 cm. The gate opening ranges from 0.5 cm to 2.25 cm, and discharge ranges from 11.5 L/s to 41 L/s. In the second category the water head upstream the sluice gate ranges from 76 cm to 81 cm. The gate opening ranges from 1.4 cm to 2.5 cm, and flow discharge ranges from 23 L/s to 41 L/s. The third category of the first set was carried out under upstream water head ranges from 59 cm to 61 cm, and gate opening ranges from 2.5 to 3.5 cm. The flow discharge ranges from 32 L/s to 41 L/s.

In the second set of the experiments, the bed downstream the solid apron was replaced by another bed with median diameter of 14 mm. The second set has thirteen run through three categories. The three categories are carried out under upstream water heads of 109

cm, 72-78 cm, and 56-59 cm, respectively. The gate opening ranges from 1.25 to 3.4 cm, and flow discharge ranges from 23 L/s to 41 L/s.

The third set of the experiments was carried on a bed of median diameter of 19.5 mm. The third set consists of 10 runs. These runs are also divided into three categories. The first category was carried out under upstream water head ranges from 104 cm to 109 cm, flow discharge from 30 L/s to 41 L/s, and gate opening of 1.6 cm to 2.25 cm. The second category consists of two runs, the first is carried out under upstream water head of 78 cm, water discharge of 32 L/s, and gate opening of 2.0 cm, while the second one is carried out under upstream water head of 72 cm, discharge of 41 L/s, and gate opening of 2.5 cm. The third category was carried out under the upstream water head of 52 cm to 59 cm, water discharge from 32 L/s to 41 L/s, and gate opening of 2.5 to 3.4 cm. Each run continues five hours; the time at which the scour hole downstream the soild apron reaches to the equilibrium stage. Both the scour hole and water surface profiles are measured after each run.

ANALYSIS AND DISCUSSION OF THE RESULTS

DEVELOPMENT OF LOCAL SCOUR

Figures (2) to (8) illustrate examples of the development of the local scour downstream the solid apron of a regulator for the different flow rates, different gate openings, different values of upstream water head, and different bed material median diameter. From Figures (2) to (4), it is shown that the ultimate scour depth decreases as the upstream head decreases, with regard that both the discharge and bed material are constant. This can be attributed to the fact that the jet velocity is directly proportional with the value of upstream head, and the decrease in velocity means decrease in momentum, which responsible on carrying bed particles. It is shown that the long-term scour depth increases from Figs. (5) to (7), respectively. This can be explained as the upstream water head is approximately the same, which means that the inflowing water velocity has the same value, but the water discharge increases from Fig. (5) to Fig (7), respectively, which increases the inflowing water momentum. This leads to an increase in the scour hole depth and volume. It can be also seen from figures that the hump height increases with the decrease of the discharge under the constant upstream water head. This can be explained as the decrease of discharge decreases the inflowing water momentum, which decreases its carrying capacity. From these figures, it is generally shown that the scour hole formed downstream the solid apron decreases with the increase of bed material median diameter. Also, the downstream slope of the scour hole is less flatter in runs of bed material median diameter of 19.5 mm than the corresponding ones in runs of median diameter of 14.0 mm and 10.0 mm, respectively. This can be explained due to the fact that the inflowing water momentum is not able to move the big particles away as in the small ones.

MODEL VERIFICATION

In 1965 Egiazaroff [1] proposed an equation for the incipient motion for the nonuniform particles as:

$$\tau_c / (\gamma_s - \gamma) D_{50} = \frac{0.1}{\left[\log 19 \frac{D_{50}}{D^-}\right]^2} \tag{24}$$

From the theoretical study, it can be concluded that:

$$\frac{d_s}{Y_a} = \sqrt{\frac{C_2}{C_1 C_s}} \frac{U_a}{\sqrt{(S_s - 1) D_g g}} \tag{25}$$

In the following study for D_{50} =0.01 m, D^-=0.0097 m, and from Equation (24) the Shields parameter is $\tau_c / (\gamma_s - \gamma) D_{50}$= C_s = 0.057. The value of C_1=ds/Ls, which depends on the maximum depth of the scour hole and the distance of this depth from the apron. From experimental results it can be concluded that the value of C_1 ranges between 0.2 to 0.26. From this study it can be concluded that C_1 = 0.23, C_s= 0.06, and C_2 depends on the velocity and the water depth at the end of the apron, as well as the distance of the section of the maximum scour depth from the end of apron. From the theoretical study C_2 =0.25ν /U_a Y_a.

The mathematical model is verified using the data resulted from the laboratory work through three sets of the experiments as illustrated in computer program represented in Appendix. The results of the computer model are compared by the corresponding laboratory results. From Figures (9) to (11), it is evident that the results from the mathematical model are very close to those resulted from the experimental work for different bed material median diameter.

FACTORS AFFECTING ON THE LONG-TERM SCOUR

A- Effect of upstream water head

From Figures (2) to (4), it is clear that both the scour hole profile and the volume of the transported material from the scour hole for the cases of the same boundary conditions increase with the increase of the upstream water head. This can be explained due to the fact that the increase of the upstream water head increases the inflowing velocity. The increase of water velocity with the same discharge increases the water momentum, which increases the ability of water to carry the bed particles from the scour hole.

B- Effect of the discharge

Figures (5) to (7) show that the increase in discharge with constant upstream head and bed material increases the long-term scour depth. This can be explained due to the fact that the increase of discharge increases the momentum of the inflowing water, which

increases the ability of the water to transport the bed material from the scour hole. The aforementioned trend is also evident for the bed material median diameter of 10 mm, and 19.5 mm for different values of the upstream water head.

C- Effect of the gate opening

From figures, it is evident that the maximum scour depth increases with the increase of the gate opening provided that the other factors affecting on the long-term scour depth are constant. This due to the increase of gate opening with a constant upstream water head increases the discharge, which can be explained as in article B.

D- Effect of bed material median diameter

From Figures it can be concluded that the long-term scour depth decreases with the increase of bed material median diameter, d50. This can be explained due to the fact that the inflowing water with constant momentum is able to convey the small particles away than the big ones.

CONCLUSION

The research aims to the determination of the long-term scour characteristics downstream regulator structures at the refilling of canals. In the present study the gravel is used as a bed material, whereas the using of the natural bed material (silt, clay, or sand) under high values of Froude number in the recirculating flume will damage the pump vans due to the transportation of the bed material to the pump intake. The theoretical and experimental studies suggest the following conclusions:

1- Long-term scour depth depends mainly on the jet diffusion characteristics, Shields parameter, Reynolds number, and densemeteric Froude number.
2- A mathematical model is developed to calculate the maximum scour depth, its location from the apron of the regulator, and the total length of the scour hole formed directly downstream the solid apron of the regulator at various operating conditions and different channel bed material median diameters.
3- It is evident that the results resulted from the mathematical model are very closed to that resulted from the experimental work for different bed material median diameters.
4- The effects of the various operating conditions such as, the upstream water head, the inflowing discharge, the gate opening, and the median diameter of the bed material are taken into account as follows:
    A- The long-term scour depth increases with the increase of the upstream water head provided that the remaining factors affecting on the long-term scour depth are constant.
    B- The long-term scour depth increases with the increase of the discharge.
    C- The maximum scour depth increases with the increase of the gate opening. This is applicable for different upstream water heads, and different bed material median diameters.

D- The increase of bed material median diameter results in a decrease in the long-term scour depth.

5- The downstream slope of the scour hole decreases as the bed material median diameter increases.

REFERENCES

1- Egiazaroff, I. V., 1965 "Calculation of nonuniform sediment concentration," J. of the Hydraulic Division, ASCE, Vol. 91, No. HY4.

2- El-Alfy K. S., 1995 "Long-term erosion around control structures" Ph.D. Thesis, Civil Engineering Department, Faculty of Engineering, University of Menufia, Shebin-El Kom, Egypt.

3- Hoffmans, G. J. M., 1988, "Flow simulation by the two-dimensional turbulence model" Rep. 2-88, Hydr. Geotechn. Eng. Div., Delft Univ. of Technology, Delft.

4- Kramer, H. 1934 "Sand mixtures and sand movement in fluvial models", ASCE. Vol. 100, pp. 798-878.

5- Kamel, S., 1992 "Effect of supercritical flow on riprap protection downstream weir structures", thesis presented to the Univ. of Ain Shams, Cairo, Egypt, in partial fulfillment of the requirement of the degree of Doctor of Philosophy in Eng.

6- Melville, B. W., 1975, "Local scour at bridge sites" thesis presented to the Univ. of Auckland at Auckland, New Zealand, in partial fulfillment of the requirement of the degree of Doctor of Philosophy in Eng.

7- Melville, B. and A. J. Raudkivi, 1977 "Flow characteristics in local scour at bridge piers", J. Hydr. Res. 15: 373-380.

8- Mohamed, M. S. 1990 "Erosion prediction and control in irrigation canals" Partial Fulfillment of the requirements for the degree of Doctor of Philosophy, University of Windsor, Windsor, Ontario, Canada.

9- Mtller, R., 1947 "Die Kolkbildung beim renen unterstromen und allgemeinere Behandlung des Kolkproblemes", Mitt. Versuchsanstalt ftr Wasserbau ETH Ztrich Nr. 5.

10- Schoklitch, A., 1914 "Ueber Schieppkraft und Geschiebe bewegung", Engelmann, Leipzig (in German).

11- Simons, D. B. and Senturk, F., 1976 "Sediment Transport Technology", Water Resources Publications, Littleton, Colorado.

NOTATION

The following symbols are used in this paper:

C_1	lift coefficient
C_2	hydrodynamic resistance coefficient of the sediment
C_3	form coefficient related to the volume of particle
C_4	form coefficient related to the effective surface of the particle
C_5	form coefficient defining the effective surface of the particles
C_L	lift coefficient
C_s	Shields parameter
Dg	grains diameter
d_{50}	median diameter of grains
D^-	average diameter of grains
d_s	long-term scour depth
g	gravity acceleration
G	gate opening
H	upstream water head
K	constant determined from laboratory measurements
L	apron length
L_s	total length of the scour hole
L_{sm}	distance between the end of the apron and the section of the maximum scour depth
Q	discharge liter/sec.
S_s	specific gravity of sediment particles
X	distance from the gate
Y_a	flow depth at the end of the apron
U_*	shear velocity
U_a	velocity at the end of the apron
U_m	maximum velocity at the maximum scour location
U_{av}	average velocity at the maximum scour location
ρ	mass density of fluid
ρ_s	particle density
γ	specific weight of fluid
γ_s	specific weight of solid particles
ν	kinematic viscosity of the fluid
τ_0	bed shear stress
μ	dynamic viscosity of the fluid
ε_m	eddy dynamic viscosity
θ	angle of repose of the particles
ϕ	angle of bed slope

APPENDIX

Flow chart of the computer program

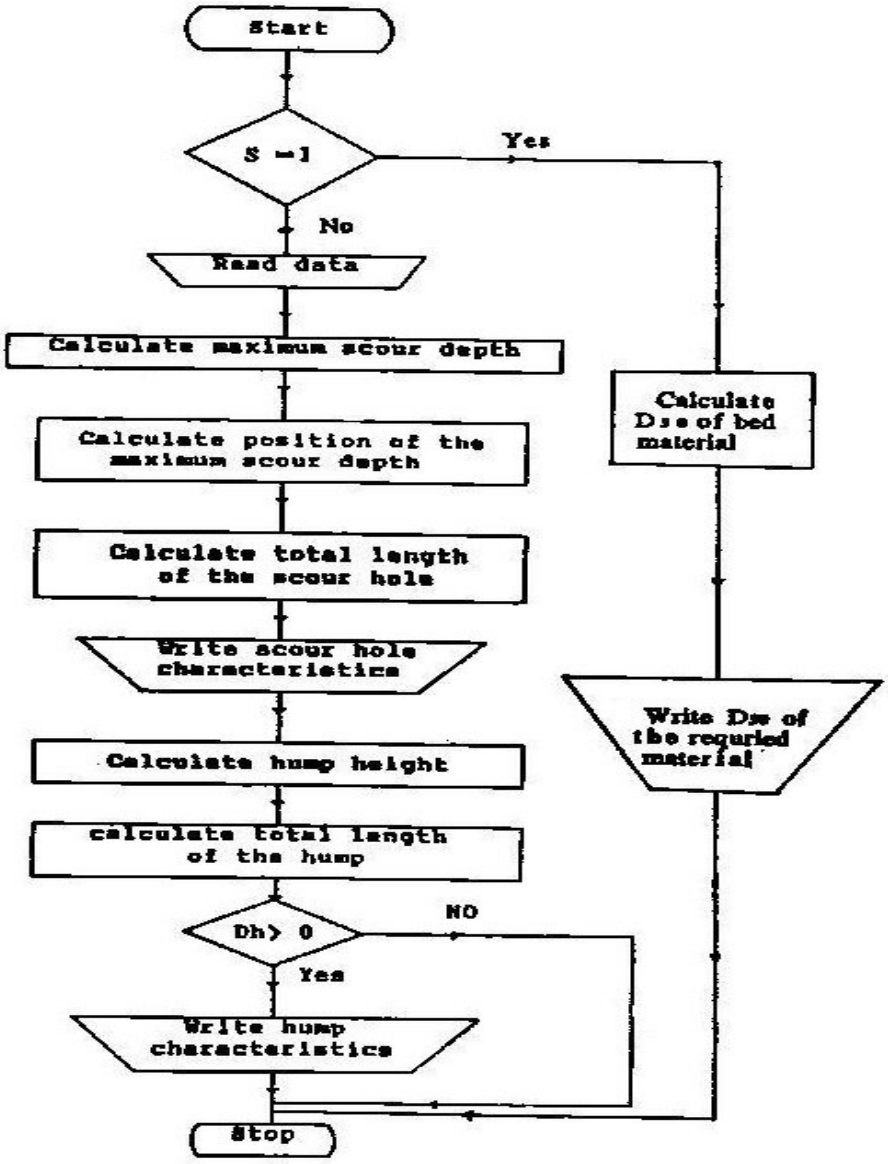

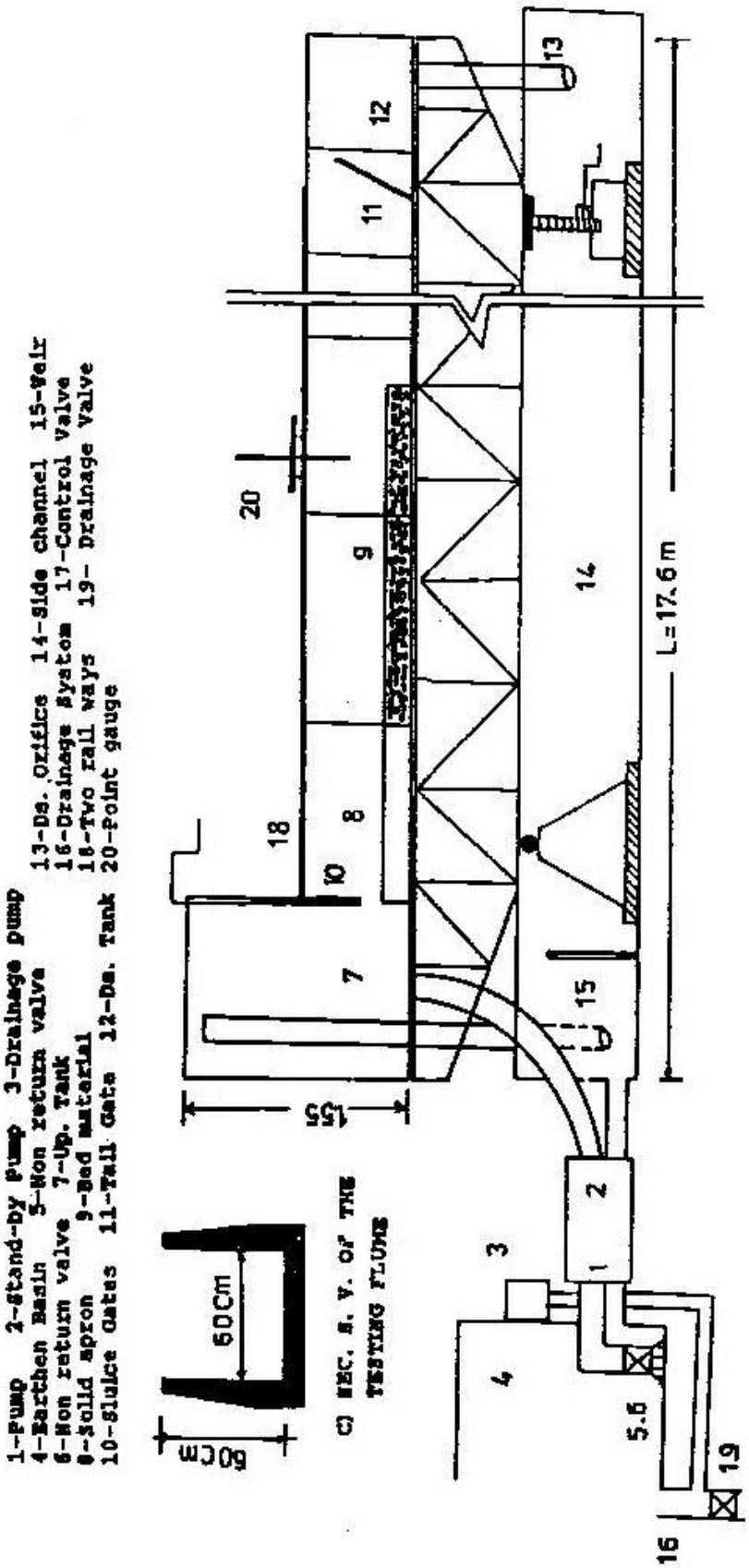

Figure (1) Elevation view for laboratory flame

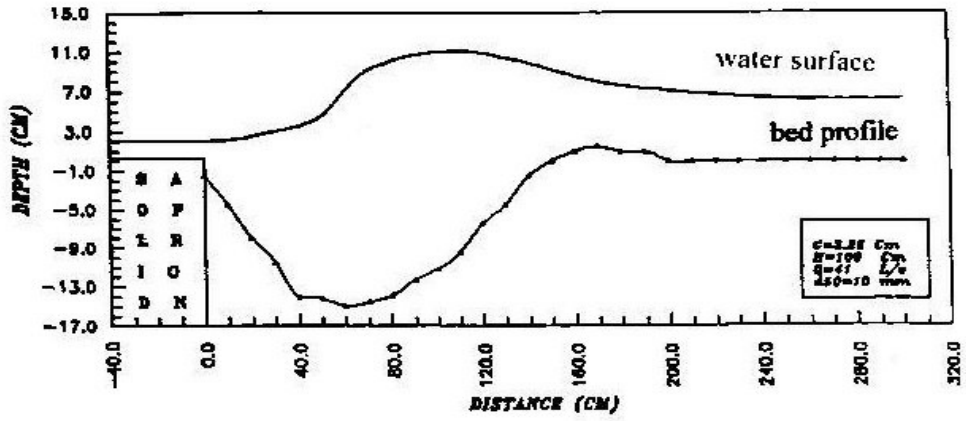

Figure (2) Variation in scour depth versus distance

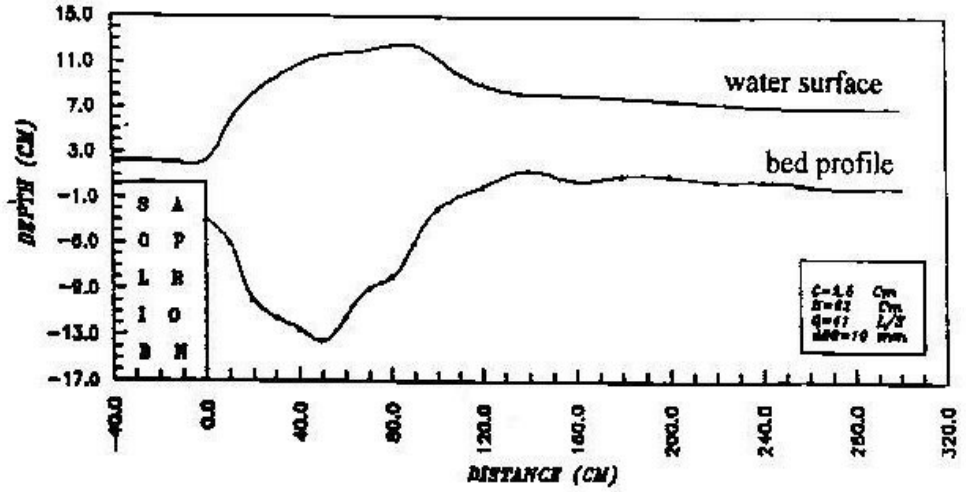

Figure (3) Variation in scour depth versus distance

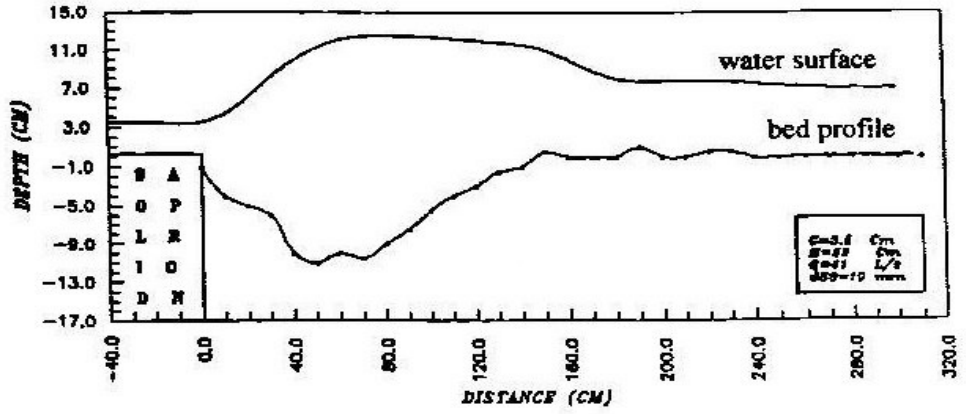

Figure (4) Variation in scour depth versus distance

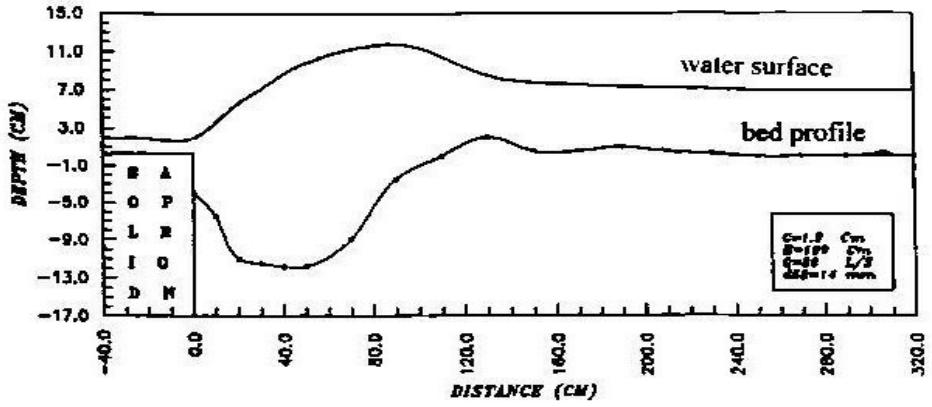

Figure (5) Variation in scour depth versus distance

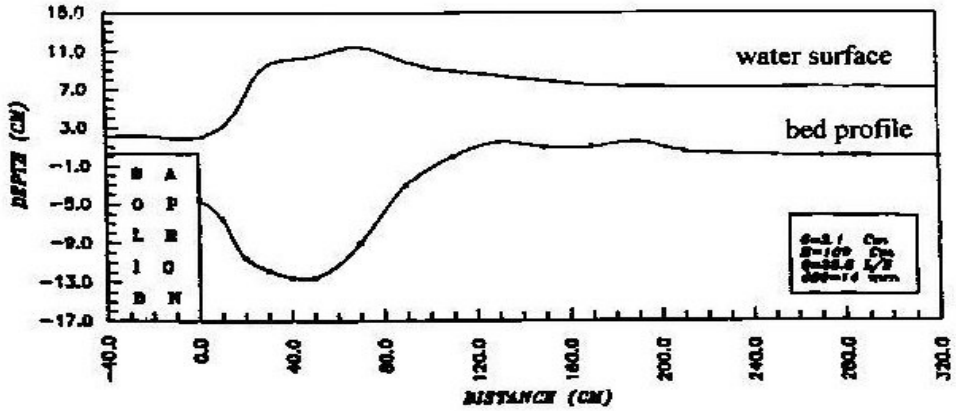

Figure (6) Variation in scour depth versus distance

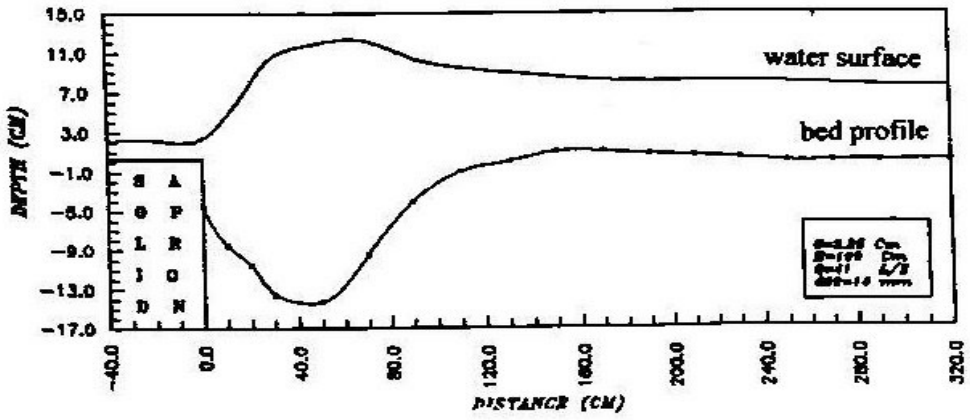

Figure (7) Variation in scour depth versus distance

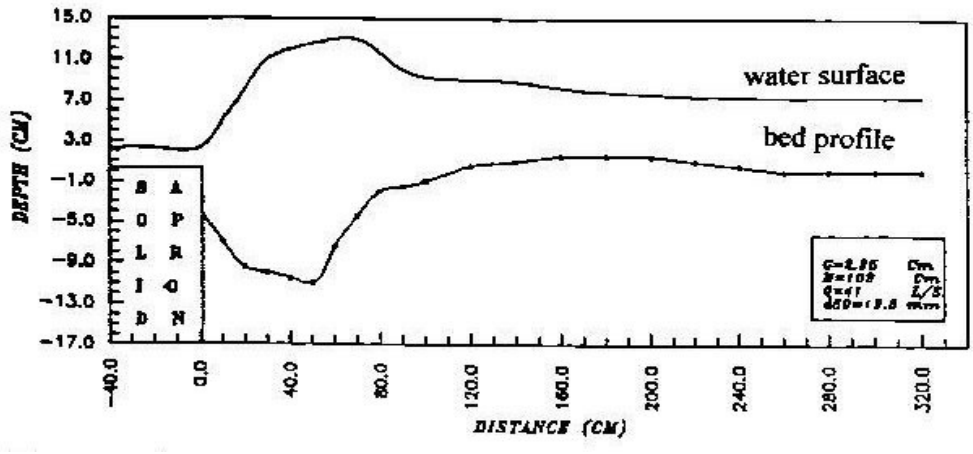

Figure (8) Variation in scour depth versus distance

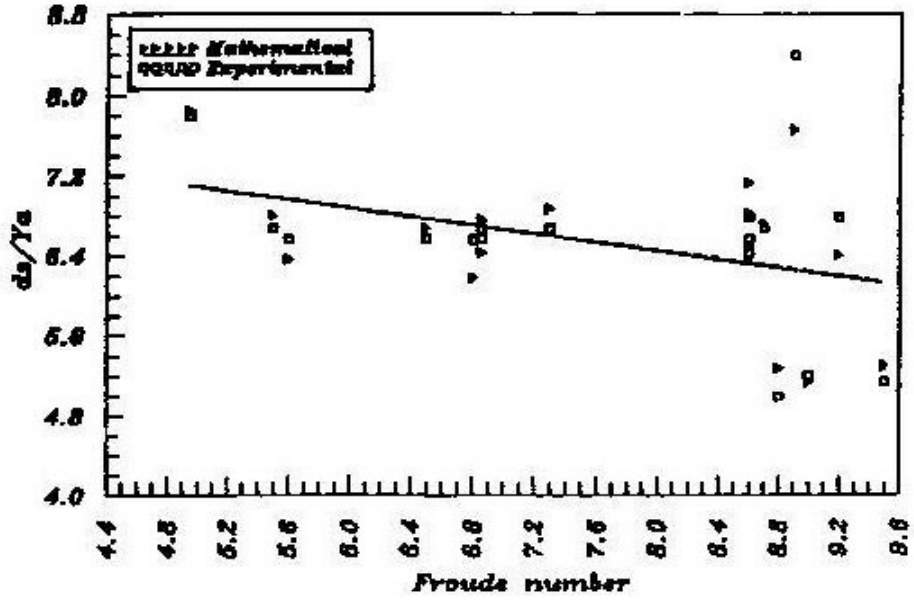

Figure (9) Comparison between mathematical and experimental dimensionless scour depth versus Froude number for bed material of d_{50} = 10.0 mm

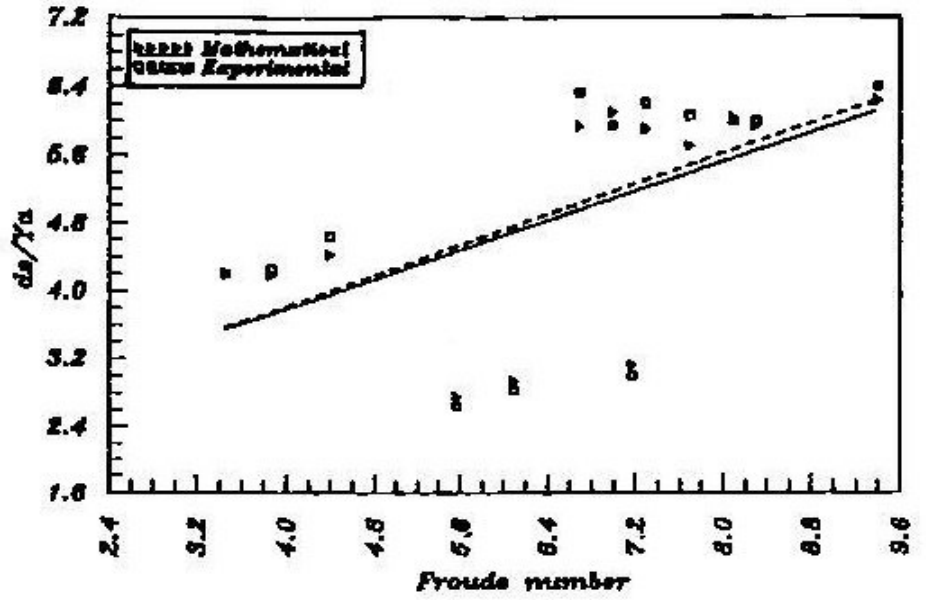

Figure (10) Comparison between mathematical and experimental dimensionless scour depth versus Froude number for bed material of d_{50} = 14.0 mm

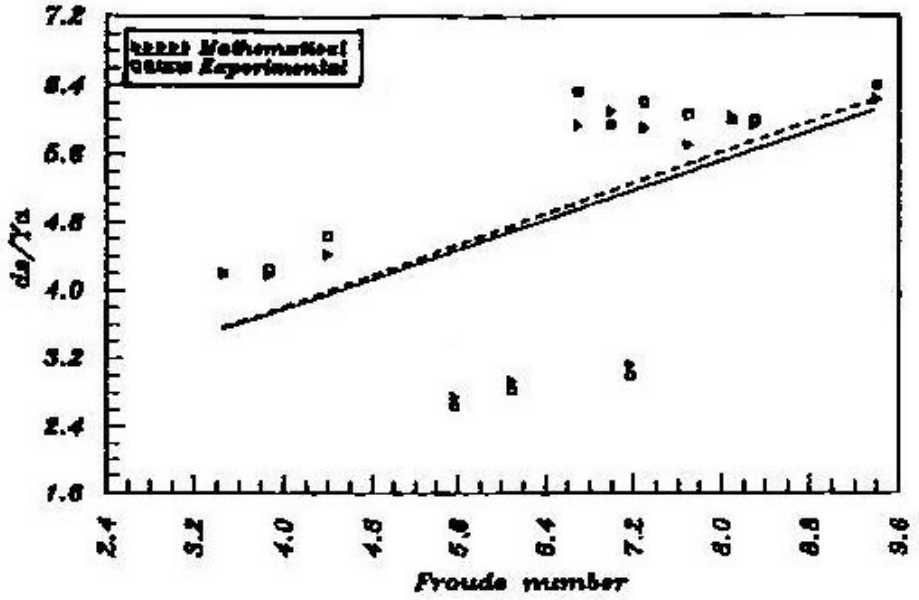

Figure (11) Comparison between mathematical and experimental dimensionless scour depth versus Froude number for bed material of d_{50} = 19.5 mm